Small RNA-seq analysis of extracellular vesicles from porcine uterine flushing fluids during peri-implantation

Renwu Hua
Huazhong Agriculture University
Yueying Wang
Jining No 1 People's Hospital
Weisi Lian
Huazhong Agriculture University
Wenchao Li
Huazhong Agriculture University
Yu Xi
Huazhong Agriculture University
Songyi Xue
Huazhong Agriculture University
Tingting Kang
Huazhong Agriculture University
Minggang Lei (leimg@mail.hzau.edu.cn)
Huazhong Agricultural University https://orcid.org/0000-0001-7515-6497

Research article

Keywords: uterine flushing fluids, extracellular vesilcles, sequencing, microRNA, Piwi-interacting RNAs, implantation

Posted Date: December 11th, 2019

DOI: https://doi.org/10.21203/rs.2.12869/v3

Version of Record: A version of this preprint was published at Gene on January 1st, 2021. See the published version at https://doi.org/10.1016/j.gene.2020.145117.

Abstract

Background: The extracellular vesicles (EVs) of uterine flushing fluids (UFs) mediate intrauterine communication between conceptus and uterus in pigs. The small RNAs of UFs-EVs are widely recognized as important factors that influence embryonic implantation in humans, mice, cattle and sheep. Therefore, it can be hypothesized that small RNAs of UFs-EVs are essential for implantation in pigs. Results: Cup-shaped EVs of porcine UFs were isolated and characterized, and then PKH67 stained extracellular vesicles were taken up by endometrial epithelial cells and porcine trophectoderm cells in a time-dependent manner. The expression of small RNAs in these EVs on days 10 (D10), 13 (D13) and 18 (D18) of pregnancy was comprehensively profiled through sequencing. From nine libraries, a total of 152 known microRNAs (miRNAs), 43 novel miRNAs and 6248 known Piwi-interacting RNAs (piRNAs) and 110 novel piRNAs were identified. Hierarchical cluster analysis and principal component analysis suggested that the expression profiles of small RNAs in D13 group were different from those in D10 and D18 groups. Bioinformatics analysis showed that the miRNAs differentially expressed in the comparisons between D10 and D13, D13 and D18, and D10 and D18 groups were involved in important processes and pathways related to immunization, proliferation, angiogenesis, apoptosis and development, which play important roles in embryonic implantation. Conclusions: Our results reveal that EVs from porcine UFs contain various small RNAs with potentially vital effects on implantation. This research also provides resources for studies of miRNAs and piRNAs in the cross-talk between embryo and endometrium.

Background

Previous studies have indicated that the majority of pre-natal losses occur during the peri-implantation period in pigs [1, 2]. During this period, the porcine blastocyst expands from 0.5–1 mm in diameter at hatching to 2-mm spheres on day 10 of pregnancy (D10) and begins to rapidly elongate into tubular and filamentous shapes on day 11 or 12 [3, 4]. The conceptus starts to attach to the surface of maternal endometrium at day 13 of pregnancy (D13) and the attachment is usually completed between days 18 (D18) and 24 of pregnancy [5, 6]. The synchronous communication between conceptus and uterus exerts strong influence on embryo implantation [7]. Furthermore, the extracellular vesicles (EVs) of uterine flushing fluids (UFs) are capable of mediating embryo-endometrium cross-talk during implantation [8, 9]. Therefore, in order to improve the rate of successful implantation in pigs, it is necessary to investigate the mechanism by which intrauterine EVs regulate the cross-talk.

EVs, including exosomes (40-120 nm) and microvesicles (100-1000 nm), can carry and transport biological information such as small non-coding RNAs, mRNAs and proteins [8, 10, 11], and they are present in saliva, plasma, milk, urine, semen, uterine flushing fluids and other biological fluids [12–15]. Moreover, these EVs have been isolated and characterized from the UFs in human [16], mice [17], cattle [18, 19], sheep [20] and pig[21]. At present, research on intrauterine UFs is still in its early stage, especially for pigs.

Small non-coding RNAs mainly include three classes: microRNAs (miRNAs), Piwi-interacting RNAs (piRNAs) and small-interfering RNAs (siRNAs) [22]. Among these small RNAs, miRNAs are single-stranded and non-coding RNAs consisting of 18–24 nucleotides [23]. They can regulate gene expression at the post-transcriptional level and participate in many biological processes, including apoptosis, cell differentiation, cell proliferation, and tumorigenesis [24]. The piRNAs are small non-coding RNAs associated with PIWI family proteins that silence transposable elements in the animal germline [25]. The interference of siRNA on gene expression is considered as a naturally occurring biological strategy for silencing alleles in vertebrates [26]. Previous studies have indicated that small RNAs such as miR-21-5p [27], miR-30d [28], miR-26a [29] and let-7a [30] play vital roles in embryo implantation. Despite their acknowledged importance, the biological function and significance of small RNAs in implantation have not been fully elucidated.

In this study, UFs-EVs of gilts were isolated and characterized, and then the expression of small RNAs in these extracellular vesicles was profiled on days 10, 13 and 18 of pregnancy, aiming to provides a resource for studies of miRNAs and piRNAs in communication between embryo and endometrium.

Results

Characterization of extracellular vesicles from porcine UFs

Extracellular vesicles were obtained from porcine UFs by filtration and ultracentrifugation. Western Blot (WB) analysis revealed that the UFs-EVs fraction was positive for exosome-related protein markers (CD63, CD9 and HSP70) and negative for cytochrome C and calnexin (Figure 1A). The cup-shaped UFs-EVs were observed by transmission electron microscope (TEM) (Figure 1B). In addition, separated UFs-EVs were subjected to nanoparticle tracking analysis (NTA), revealing that their sizes ranged from 40 to 160 nm (Figure 1C). Results from Agilent 2100 Bioanalyzer show that the RNA content and RIN/RQN value of UFs-EVs are 2.63±0.78 ng/μL and 2.6±0.2, respectively. RNase treatment result in an absence of miRNA, meaning that EVs protected miRNAs from degradation (Figure 1D).

Then, we tested whether porcine UFs-EVs can be taken up by endometrial epithelial cells (EECs) and porcine trophectoderm porcine trophectoderm cells (PTr2). These porcine UFs-EVs (20 μg/mL) were labeled with the fluorescent dye PKH67 and added into the culture medium of EECs or PTr2 cells for 12 h or 24 h. PKH67 labeled UFs-EVs were successfully internalized by EECs and PTr2 cells in a time-dependent manner. Relative green fluorescenc

e emitted by the UFs-EVs was used to assess the amount of EV uptake. The results suggested that there was significant increase in the relative fluorescence indicating an increased uptake over a period of time in EECs group (Figure 2A, C). However, there was significant reduction in the relative fluorescence indicating the disappearance of UFs-EVs in the PTr2 cells over a period of time in PTr2 cells group (Figure 2B, D).

Small RNA sequencing data

Nine small RNA-seq libraries of porcine UFs-EVs were generated from nine gilts on days 10, 13 and 18 of pregnancy. The length distribution of reads showed that the highest peak was at 22 nucleotides (nt), which was consistent with the expected length of miRNAs. It is worth noting that the second peak appeared in the length range of 28–33 nt, which might correspond to piRNAs (Figure 3). Altogether, we obtained 297,715,036 raw reads and 209,120,304 clean reads (Additional file 1: Table S1). Among the clean reads, known miRNAs (17.67%) and piRNAs (48.69%) were identified, while 0.84% and 1.31% of clean reads were aligned to novel miRNAs and piRNAs, respectively (Additional file 2: Figure S1).

Then, quantitative PCR (qPCR) was performed on 16 chosen differently expressed small RNAs, including five known miRNAs, five novel miRNAs, three known piRNAs and three novel piRNAs, to verify the reliability of the sequencing data. All Pearson correlation coefficients between the qPCR data and sequencing data were greater than 0.7, indicating that the expression patterns of miRNAs and piRNAs determined by qPCR were generally consistent with those obtained by sequencing (Table 1).

Prediction of miRNA target genes

Piano and miRNADeeps2 were used to predict novel piRNAs and miRNAs, respectively. We normalized the relative expression levels of miRNAs to TPM. After filtering (TPM >28 in at least one library), we identified 152 known miRNAs, 43 novel miRNAs, 6248 known piRNAs and 110 novel piRNAs (Additional file 3: Table S2). The target genes of the miRNAs are shown in Table S4, which were derived from the intersection of miRnada, RNAhybird and Targetscan predictions (Addition file 4: Table S3).

Clustering analysis

To explore the differences in small RNA expression pattern of the porcine UFs-EVs during different phases of peri-implantation, hierarchical cluster analysis (HCA) was preformed to cluster these miRNAs and their expression profiles in the three stages with 43 novel miRNAs and 152 known miRNAs. The results revealed that the expression profiles of small RNAs in D13 group were different from those in D10 and D18 groups (Figure 4). The results also showed that these miRNAs were grouped into 3 categories: category A (e.g., ssc-let-7a), category B (e.g., ssc-let-7c, ssc-miR-30d, ssc-miR-21-5p) and category C (Figure 4). In addition, the expression patterns of the small RNAs at three stages were investigated by principal component analysis (PCA). The results indicated that samples of the same stage were clustered together (Additional file 5: Figure S2).

Functional annotation of target genes of highly expressed known miRNAs

To determine whether the expression of miRNAs in porcine UFs-EVs is related to that of miRNAs in endometrium and embryos during peri-implantation period, the expression of top 20 highly expressed known miRNAs in UFs-EVs was compared with that in embryos at D10, endometrium at D10 and endometrium at D12 [31–33]. The results indicated that most of these miRNAs were expressed in both the embryo and endometrium (Additional file 6: Table S4). Importantly, ssc-miR-21-5p was the most highly differently expressed miRNA in porcine embryos, endometrium and UFs-EVs, and ssc-let-7a, ssc-let-

7g, ssc-let-7f-5p, ssc-let-7i-5p, ssc-miR-26a and ssc-miR-429 were also highly expressed (Figure 5). The predicted target genes of these miRNAs were used for functional analysis. Gene Ontology (GO) analysis (ClueGo network of GO terms) indicated that the target genes were mainly involved in “G protein-coupled receptor signaling pathway”, “cell differentiation”, “cell-substrate adhesion” and “cell surface receptor signaling pathway” (Figure 6). Kyoto Encyclopedia of Genes and Genomes database (KEGG) analysis showed that they were mainly enriched in “Cell cycle”, “mTOR signaling pathway”, “Insulin signaling pathway”, and “Progesterone-mediated oocyte maturation” (Additional file 7: Table S5).

Identification of differentially expressed small RNAs

We compared the expression of small RNAs on D10, D13 and D18 of pregnancy with each other (D10 vs D13, D13 vs D18 and D10 vs D18). Small RNAs (TPM >28 in at least one library) with P-values <0.05 and foldchange ≥2 as differentially expressed (DE) small RNAs (Additional file 8: Table S6). As a result, 172 DE miRNAs and 5602 DE piRNAs were obtained. It is noteworthy that 55 DE (e.g., ssc-let-7a) miRNAs and 2407 DE piRNAs were commonly found in all three comparisons (Figure 7A, B).

Time-series expression analysis

The short time-series expression miner (STEM) was used to investigate the pattern of DE miRNA expression during the three stages (Additional file 9: Table S7). The typical expression pattern (P<0.05) was profile 6 (Figure 8B, Additional file 10: Table S8) and profile 5 (Figure 8C, Additional file 11: Table S9). Expression of 51 miRNAs (e.g., ssc-let-7a, ssc-let-7f-5p, ssc-let-7i-5p, ssc-let-7g) assigned to profile 6 which first increased from D10 to D13 and then stay stable until D18 (Figure 8B). In addition, 36 miRNAs were enriched in profile 5 (e.g., ssc-miR-21-5p and ssc-miR-26a), and the expression levels of these miRNAs reached the peak on D13 and significantly decreased thereafter (Figure 8C). Notably, Profile 6 and profile 5 have the same in that miRNA expression level elevated from D10 to D13.

Functional annotation of predicted target genes of DE miRNAs

To analyze the functions of DE miRNAs in porcine UFs-EVs during peri-implantation, GO and KEGG analyses were performed on the predicted target genes of these miRNAs in three comparisons (D10 vs D13, D13 vs D18 and D10 vs D18). Significantly enrichment GO terms mainly included “cell cycle”, “immune effect process”, “regulation of transcription by RNA polymerase II”, “Ras protein signal transduction”, “G-protein coupled receptor activity” and “DNA binding” in all three comparisons (Figure 9). The KEGG analysis showed that the top20 significantly enriched pathways in three comparisons were “TNF signaling pathway” (Immunization-related pathway), “apoptosis” (Cell death-related pathway), “Axon guidance” (development-related pathway), “Phosphatidylinositol signaling system” (Signal transduction-related pathway), “Insulin resistance” and “Insulin signaling pathway” (Endocrine related pathway) (Figure 10). Notably, “AGE-RAGE signaling pathway in diabetic complications” (Angiogenesis-related pathway) was significantly enriched pathway in D10 vs D13 comparisons.

Discussion

The intrauterine EVs could mediate embryo-endometrium cross talk during embryo implantation [8]. In the present study, porcine UFs-EVs were isolated and identified through NTA, TEM and WB. A comprehensive profiling of the expression of small RNAs in these extracellular vesicles on D10, D13 and D18 was carried out via sequencing. The small RNAs (TPM >28 in at least one library) included a total of 152 known miRNAs, 43 novel miRNAs, 6248 known piRNAs and 110 novel piRNAs, among which 130, 42, 5492 and 110 were differentially expressed during the three stages. Importantly, Functional annotation of predicted target genes of highly expressed known miRNAs and DE miRNAs have been done to define the potential role of UFs-EVs miRNAs during embryo implantation.

Characterization of UFs-EVs

The UFs-EVs were identified as cup-shaped vesicles with a diameter of 40-160 nm and measurement of exosomal protein markers CD63, CD9 and HSP70 [34]. In order to test whether UFs-EVs can be transferred to EECs or PTr2 cells, we established an *in vitro* model that cell internalize labelled EVs. In our study, PKH67 labelled UFs-EVs were successfully internalized by EECs and PTr2 cells in a time-dependent manner. We concluded that UFs-EVs could be taken up by both endometrium and embryo trophoblast.

D10 Group Directly Cluster with D18 Group

In the clustering analyses, the PCA results suggested that the expression profiles of small RNAs in porcine UFs-EVs vary among different stages. HCA of miRNAs showed that D10 group was directly clustered with D18 group but not with D13 group. These results imply that the expression profiles of small RNAs in porcine UFs-EVs vary significantly from D10 to D13, possibly because of the constant elongation and subsequent attachment of blastocysts to the surface of endometrium during this period.

Highly Abundant miRNAs Might Influence Endometrial Receptive and Embryo Development

Previous studies have shown that highly expressed miRNAs may play vital roles in the regulation of embryo implantation [35, 36]. The expression of top 20 most highly expressed known miRNAs in UFs-EVs was compared with that in endometrium at D10 or D12 and embryo at D10 [31–33]. Among these miRNAs, ssc-miR-21-5p was the most abundant in all libraries. MiR-21-5p was also found in ovine mammary gland [37] and milk [38] during early pregnancy. MiR-21 (miR-21-5p) in extracellular vesicles is conducive to embryo development and prevention of high embryo death rate in mice [39]. Moreover, ssc-miR-21-5p, ssc-let-7a, ssc-let-7i-5p and ssc-let-7g were highly expressed in the endometrium during per-implantation in Meishan and Yorkshire pigs [36]. A previous study also indicated that let-7a alters miRNA expression to influence the implantation competency of the activated blastocysts by regulating Dicer expression [30]. Other studies indicated that miR-26a influence endometrial receptivity by targeting PTEN in dairy goats[29], and miR-429 suppresses epithelial-mesenchymal transition (EMT) *in vivo* and *in vitro* via targeting protocadherin 8 during embryo implantation in mice [40]. The ClueGO analysis of highly expressed known miRNAs indicated that the predicted target genes were enriched in biological processes and molecular functions associated with blastocyst activation (e.g., “G protein-coupled receptor signaling pathway”), embryo development(e.g., “cell differentiation”) and endometrial receptivity (e.g., “cell-

substrate adhesion" and "cell surface receptor signaling pathway") [41, 42]. Notably, a previous study has suggested that G-protein coupled receptor may play a vital role in embryo-maternal crosstalk during the period of maternal recognition and establishment of pregnancy [43]. Both previous research and our results reveal that these most highly abundant miRNAs in porcine UFs-EVs may act on regulating embryo development and endometrial receptivity at the time of implantation.

DE miRNAs Related to Proliferation, Immunization and Angiogenesis

Of 172 DE miRNAs in three comparisons, 18 DE miRNAs (e.g., ssc-miR-30d, ssc-miR-125b, ssc-miR-200b) were observed for D10 vs D13 and for D13 vs D18 comparisons, and 50 DE miRNA (e.g., ssc-miR-451, ssc-miR-181c, ssc-let-7i-5p) were observed for D10 versus D13 and for D10 versus D18 comparisons. In these miRNAs, a previous study indicated that miR-451 and its target Ankrd46 have effect on embryo implantation in mice [44]. It was also shown previously that downregulation of miR-451 in mouse and human oocytes influenced pre-implantation embryogenesis via inhibiting the Wnt signaling pathway [45]. Krawczynski and coworkers [46] found that ssc-miR-125b was present in porcine UFs-EVs and could regulate expression of vital genes for establishment of pregnancy involved in immune system function, endometrial receptivity or embryo/trophoblast development and implantation. Interestingly, The expression levels of miR-451 and miR-125b in the endometrium of pregnancy woman with high progesterone levels were lower than them with normal progesterone levels [47]. In addition, the evidence has shown that miR-200b was able to induced EMT via targeting ZEB1 and SIP1 during tumour metastasis [48]. Has-miR-30d, secreted by the human endometrium, promoted embryo adhesion by regulating *Itgb3*, *Itga7* and *Cdh5* [28].

The STEM analysis showed that DE miRNAs were significantly cluster into two profiles. In these miRNAs, sssc-let-7a, ssc-let-7d-5p, ssc-let-7e, ssc-let-7f-5p, ssc-let-7g, ssc-let-7i-5p, ssc-miR-181c and ssc-miR-451 were cluster into Profile 6, while ssc-miR-21-5p, ssc-26a-5p and ssc-miR-181a were cluster into Profile5. A recent study demonstrated that let-7 family involved in the Lin28B/let-7 axis, which is the key regulatory mechanism of the immune inflammatory response during early pregnancy in cattle and the angiogenesis during the development of human malignances [49, 50]. In addition, ssc-miR-181a and ssc-miR-181c may regulate embryo implantation by targeting *SPP1* (adhesion molecule) in porcine endometrium[51]. Notably, ssc-miR-181a, ssc-miR-let-7c, ssc-miR-26a, ssc-miR-451, ssc-miR-200b, ssc-miR-21-5p, ssc-miR-30d, ssc-miR-181c, ssc-miR-429 and ssc-miR-129b were grouped into category B from HCA, which shows a high level of expression of miRNA on D13.

The successful pregnancy during peri-implantation is associated with a series of important biological processes [52]. Function annotation analysis can provide insight into of biological processes and molecular functions of target genes. The GO analysis showed that the main processes enriched in the three comparisons were associated with immune regulation (e.g., immune effect process), signal transduction (e.g., Ras protein signal transduction) and proliferation (e.g., cell cycle). In KEGG analyses, "TNF signaling pathway", "apoptosis", "Axon guidance", "Phosphatidylinositol signaling system" and "Insulin signaling pathway" were common signaling pathways in the three comparisons. Among these

pathways, axon guidance is a means of directing the axon process of differentiated nerve cells to its target during embryonic development [53]. TNF signaling pathway was associated with the regulation of apoptosis in murine blastocysts *in vitro* and *in vivo* [54]. A previous study has suggested that DE mRNAs between patient with repeated implantation failure and women who conceived after one IVF/ICSI attempt during window of implantation participated in Phosphatidylinositol signaling system [55]. In addition, activation of placental insulin signaling pathway contributes to increases in fetal growth and stimulation of placental amino acids in obese mice [56]. In another study, research data indicated that insulin signaling pathway was related to cell proliferation [57]. As to “AGE-RAGE signaling pathway in diabetic complications”, which is significantly enriched in D10 vs D13 comparisons. A previous study indicated that AGE / RAGE signaling can mediate the decline of VEGFR-2 protein and mRNA expression, leading to functional angiogenesis disorders in bone marrow-derived endothelial progenitor cells [58]. Collectively, these results suggest that DE miRNAs in porcine UFs-EVs may have effects on proliferation, immunization, angiogenesis and embryo development during embryo implantation.

Although the DE miRNAs and highly expressed known miRNAs were found and their biological functions were predicted by using bioinformatics analysis in this study, further studies are needed to definitely validate their roles in vitro. Besides small RNAs, other biological information, including mRNAs, proteins, long non-coding RNAs and circle RNAs, is also transported by extracellular vesicles of UFs and involved in the cross-talk between conceptus and endometrium. More sequencing analyses will facilitate a more comprehensive understanding of the regulatory mechanism of porcine UFs-EVs. Furthermore, The piRNAs have been found in spent culture media of embryo [59], our results shown that lots of piRNAs were present in porcine UFs-EVs. However, there are currently not enough studies on porcine piRNAs or effective methods that accurately predict their target genes in pigs, so this analysis of porcine UFs piRNAs is limited.

Conclusions

In conclusion, porcine UFs-EVs were isolated and characterized, and proved to be taken up by EECs and PTr2 cells in a time-dependent manner. The small RNA expression in these extracellular vesicles was profiled on D10, D13 and D18 of pregnancy. The target gene functional annotation indicated that these DE miRNAs may influence embryonic implantation by regulating pathways or processes related to proliferation, immunization, angiogenesis and embryo development. This research also provides a resource for studies of miRNAs and piRNAs in communication between embryo and endometrium.

Methods

Sample preparation

The animal experiment has been described in Wang et al [60]. All experiments involving animals were carried out in accordance with regulations (No. 5 proclamation of the Standing Committee of Hubei People’s Congress) approved by the Standing Committee of the Hubei People's Congress in P. R. China. All

animal sample collection procedures were approved by the Ethics Committee of Huazhong Agricultural University. The animals were housed at Jingpin farm of Huazhong Agricultural University (Wuhan, China) and were slaughtered at the slaughterhouse of Huazhong Agricultural University. Before every gilt was slaughtered, a warm shower to relax the pigs, then they were stunned with low-voltage electric shock to reduce the pain and were exsanguinated by puncturing carotid artery to death.

Nine purebred Yorkshire gilts with similar weights (120 ± 10 kg), ages (8 months) and genetic background were selected in this study. Gilts were artificially inseminated using extended semen from one boar (the breeding pig farm of Huazhong Agricultural University) at the onset of estrus (day 0) and again 12 h after. Uteri were obtained from pigs slaughtered on days 10, 13 and 18, and uterine flushing fluids (UFs) was collected by flushing with 30 mL phosphate buffer saline (PBS; pH 7.4, catalog number: 02-024-1ACS, Biological Industries). The presence of filamentous conceptuses in the flush of the uterine horns was used to confirm pregnancy. The UFs sample from pregnancy gilts were used for subsequent sequencing analysis. For characterization of extracellular vesicles from porcine UFs, three additional nonpregnant gilts (day13 of estrous cycle) with similar weights, ages and genetic background (see above) were slaughtered and their uteri were collected on day 13 after estrus. The UFs were obtained by using the above method. At the same time, these uteri were used for the separation of endometrial epithelial cells.

UFs exosome isolation

The UFs was clarified by centrifugation (2000 g for 30 min at 4°C), filtered through a 0.22 μm filter (MILLEX-GP, USA) to remove impurity. Then, these samples were ultracentrifuged at 130,000 g for 2 h at 4°C (Beckman Optima XE-90, SW32 Ti rotor, Beckman Coulter. USA). Extracellular vesicles (EVs) were re-suspended in 200 μL PBS (catalog number: 02-024-1ACS, Biological Industries) after washing with PBS (130,000 g for 2 h). Extracellular vesicles were stored at –80°C until the RNA was isolated.

Western blot (WB)

The exosomal and cellular proteins were extracted by DNA/RNA/protein Isolation Kit (catalog number: R6734-02, OMEGA). The sample was denatured by heating, separated by SDS-PAGE and transferred to a PVDF (polyvinylidene fluoride) membrane. Next, the membranes were blocked with 5% skimmed milk powder and separately probed with rabbit anti CD9 (catalog number: 20597-1-AP, Proteintech), rabbit anti HSP70 (catalog number: GB11241, servicebio), rabbit anti CD63 (catalog number: ab231975, abcam) , rabbit anti calnexin (catalog number: 10427-2-AP, Proteintech)and rabbit anti cytochrome c (catalog number: sc:13156, santa cruz) overnight at 4°C with a final dilution of 1:1000 (v/v). After three times of washing, the membranes were incubated with goat anti-rabbit secondary antibodies (catalog number: GB23303, Sevicebio) with 1:2000 dilution (v/v) at 37°C for 1.5 h. The images of membranes treated with ECL (enhance chemiluminescence) were captured by Western Blotting Detection System (Tiangen, Beijing, China).

Transmission electron microscope (TEM)

The morphology of isolated extracellular vesicles was visualized with high-resolution transmission electron microscope (Hitachi HT7700) based on a previous method [61]. In brief, the resuspended extracellular vesicles were placed on carbon-coated copper grid, and then subjected to 2% phosphotungstic acid (catalog number: DZ0035, Leagene) staining for 2 min. The excess liquid was blotted off by filter paper, and grids were allowed to dry overnight.

Nanoparticle tracking analysis (NTA)

The size distribution and concentration of isolated extracellular vesicles were analyzed by NTA with Zeta View (Particle Metrix). Isolated extracellular vesicles were diluted with particle-free PBS at the ratio of 1:200 and added into the chamber. The results of size distribution and vesicle concentrations were assessed with the software Zeta View.

RNA extraction and RNase treatment

The RNAs of EVs were extracted by miRNeasy Serum/plasma Kit (catalog number: 217184, Qiagen, German) according to manufacturer's protocol. The quantity and quality of RNA were assessed using a Small RNA kit and a Small RNA assay on an Agilent 2100 Bioanalyzer (Agilent Technologies, USA). Extracted RNA was treated with 10ng/ul of RNase A (Sigma-Aldrich) at room temperature for 30 min. and then treated RNA was assessed as above.

Cell culture

The uterus of non-pregnant gilts was opened longitudinally on a sterile clean bench. The endometrium was separated and shredded with a sterile scissor. After washing twice with PBS, the tissue pieces were incubated at 37°C for 2.5 h with collagenase I (catalog number: 17100017, Gibco) and shaken vigorously every half hour. Undigested tissue pieces were removed by screen filtration. Then, the filtrate was centrifuged at 500 g for 10 min to remove supernatant (fraction rich of endometrial stromal cells). The pellet (epithelial-rich fraction) was resuspended twice in PBS and recentrifuged (500 g, 10 min) twice. The resultant pellets containing endometrial epithelial cells (EECs) were suspended in Dulbecco's modified Eagle's medium/F-12 (DMEM/F12; 1:1) medium (Gibco, NY, USA) supplemented with 10% fetal bovine serum (Gibco) and 1% penicillin-streptomycin (Gibco, NY, USA) and cultured in 37°C and 5% CO_2 incubator. Endometrial stromal cells were further removed by 0.25% trypsin without edetic acid disodium salt (EDTA) after 2–4 d. The epithelial cells were then trypsinized with 0.25% trypsin-EDTA and placed on Cell Culture Flask (Corning, NY, USA) for subsequent experiments. Isolation and culture of porcine primary EECs referred to pervious research [60, 62].

Porcine trophectoderm cells (PTr2) were kindly provided by Mr. Jiang zongyong, Guangdong Academy of Agricultural Sciences. PTr2 cells were established from dispersed cell culture of day 12 filamentous conceptus obtained from pigs. These cells have been previously characterized for SN1/38 (porcine trophectoderm-specific monoclonal antibody) positive, cytokeratin 7 positive, vimentin negative, express fibronectin and many of the integrin subunits present in porcine trophectoderm in vivo. Detailed methods

have been published [63].These cells were cultured in DMEM-F12 (Gibco) supplemented with insulin (0.1 Units/mL; Sigma-Aldrich, German), glutamine (2 mM, Sigma-Aldrich), 1% penicillin-streptomycin and 5% fetal bovine serum (Gibco).

In order to ensure that EECs and PTr2 cells are not contaminated with mycoplasma, their spent culture media were assessed mycoplasma contamination with MycAway™ -Color One-Step Mycoplasma Detection Kit (catalog number: 40611ES25, yeasen) following the manufacturer's instructions.

PKH67 staining and Confocal fluorescence microscopy

Isolated extracellular vesicles were stained with PKH67 green fluorescent mini kit (catalog number: MINI67-1KT, Sigma-Aldrich) following the manufacturer's instructions. Briefly, extracellular vesicles and PBS (negative control) were respectively added to 1 mL Diluent C, and then incubated with 4 ul PKH67 for 4 min. At last, the mixture was closed with 2 mL 0.5% bovine serum albumin (BSA), washed once with PBS, and then ultracentrifuged at 130,000 g for 2 h at 4°C.

For visual inspection of the uptake of EVs by cells, the cells were placed on glass bottom cell culture dish (catalog number: 801001, NEST) and incubated at 37°C for 12h or 24h with 20 μg/mL of PKH67 labelled EVs. At the indicated time points, cells were fixed with 4% paraformaldehyde (catalog number: BL539A, biosharp) for 10 min followed by PBS wash three times for 5 min, and cells were permeabilized with 0.5% Triton X-100 (catalog number: ST795, beyotime) solution followed by PBS wash three times for 5 min. Next, 200 μL TRITC Phalloidin dye (catalog number: 40734ES75, yeasen) was added to the cells and allowed to incubate for 30 min followed by PBS wash three times for 5 min, and then 200 μL DAPI (catalog number: C1006, biosharp) solution was added to the cells and allowed to incubate for 10 min followed by PBS wash three times for 5 min. Finally, cells were visualized with a 63× oil immersion confocal microscope (LSM 800, Zeiss). The acquired images were further processed with ZEN 2.3 software.

Small RNA sequencing

Nine small RNA libraries were generated under standard procedures at Beijing Genomics Institute (BGI, China) according to a previous study [64]. Sequencing of the libraries was carried out with the BGISEQ-500 platform (BGI, China; http://www.seq500.com/en/).

Prediction of novel miRNAs, novel piRNAs and miRNA target genes

Before data analysis, clean reads were obtained by eliminating low-quality reads, adaptors, and other contaminants. Clean reads were then mapped to reference genome and other sRNA databases by Bowtie2 [65]. Because each unique small RNA was supposed to be mapped to only one category, we followed a precedence rule of MiRbase > piRBase > snoRNA (human/plant) > Rfam > other sRNA. Piano [66] and miRNADeeps2 [67] were used to predict novel piRNAs and miRNAs, respectively. This algorithm of Piano is based on the Support Vector Machine (SVM) algorithm and transposon interaction information. The miRNA expression profiles were normalized by transcript per million (TPM), as

previously reported [68]. The miRNAs with expression values of >28 TPM in at least one of the 10 libraries were selected for all the following analyses.

Prediction of the target genes of miRNAs was carried out by TargetScan, RNAhybrid and miRnada. the intersection of miRnada, RNAhybird and Targetscan predictions were selected for further analysis. The default parameters are as follows: “-en -20 -strict” (miRanda), “ -b 100 -c -f 2,8 -m 100000 -v 3 -u 3 -e -20 -p 1 -s 3utr_human” (RNAhybrid) and “the 2-8nt of 5 'end of small RNA as seed sequences and 3'-UTR region of porcine transcript were used for prediction” (Targetscan).

Differentially expressed (DE) small RNAs

The expression levels of small RNAs were calculated by using Transcript Per Kilobase Million (TPM) as described in a previous report [69]. Small RNAs with expression value >28 TPM in at least in one of the nine libraries were selected for subsequent data analysis [68]. Raw P-value were convert to adjusted P-value using the Benjamin-Hochberg false discovery rate [70]. To improve the accuracy of the identification of DE small RNAs, we defined a miRNA as a DE miRNA when reads number foldchange ≥ 2 and P-value ≤ 0.05.

Real time quantitative PCR (RT-qPCR)

First-strand cDNAs of small RNAs were synthesized by Mir-X™ miRNA First Strand Synthesis kit (TaKaRa, Dalian, China) according to the manufacturer’s instructions. The qPCR was carried out by using SYBR Green PCR Master Mix (TaKaRa, Dalian, China) and LightCycler 480II Real-Time PCR System. The forward primers of small RNAs were designed based on the mature sequences of small RNAs (Additional file 12: Table S10), and the reverse primer was a universal primer supplied by the above kit. The expression levels of small RNAs were normalized with U6 to obtain the relative expression by comparative CT method.

Hierarchical cluster analysis (HCA)

The expression values of the miRNAs (>28 TPM in at least one library) were normalized by using the Z-score. HCA was conducted using the R package.

Principal component analysis (PCA)

The expression values of the small RNAs (> 28 TPM in at least one library) were normalized by using the lg (TPM). PCA was performed using the imageGP (http://www.ehbio.com/ImageGP/index.php/Home/Index/PCAplot.html).

Functional annotation of the predicted target genes

Functional analyses of the predicted target genes were conducted on the basis of Kyoto Encyclopedia of Genes and Genomes database (KEGG) and Gene Ontology slim database (GO-slim) by using KOBAS (http://kobas.cbi. pku.edu.cn/) and PANTHER (http://www.pantherdb.org/), respectively. An enriched

functional class with a P-value <0.05 was defined as a significantly enriched target gene candidate. The network of GO terms based on the GO database was constituted by ClueGO, which is a plugin in Cytoscape (http://www.cytoscape.org/).

Time-series expression analysis

The profiles of DE miRNAs over time were visualized by Short Time-series Expression Miner v 1.3.8 (STEM, http://www.cs.cmu.edu/~jernst/stem/). The maximum number of model profiles and the maximum unit change in model profiles between time point were adjusted to 20 and 1, respectively. The STEM clustering method was selected as clustering method and other parameters were set as default. The miRNA expression profiles were ordered by significance.

Statistical analysis

Calculate the significance of relative fluorescence was assessed by two sets of comparisons using the Bonferroni t-test in SAS 9.1, and shown as * $p < 0.05$ and ** $p < 0.01$. Correlation tests were performed to calculate the correlation between the results of RNA-seq and qPCR.

Abbreviations

UFs: uterine flushing fluids; EVs: extracellular vesicles

EECs: endometrial epithelial cells; PTr2: porcine trophectoderm cells;

D10: Day 10 of pregnancy; D13: Day13 of pregnancy; D18: Day18 of pregnancy; miRNAs: microRNAs; piRNAs: piwi-interacting RNAs;

siRNA: small-interfering RNAs; PCA: principal component analysis;

HCA: hierarchical cluster analysis; WB: Western blot;

PVDF: polyvinylidene fluoride; TEM: transmission electron microscope;

NTA: nanoparticle tracking analysis; DE: differentially expressed;

RT-qPCR: Real time quantitative PCR;

KEGG: Kyoto Encyclopedia of Genes and Genomes; GO: Gene Ontology;

STEM: Short Time-series Expression Miner.

EMT: epithelial-mesenchymal transition; PBS: phosphate buffer saline

Declarations

Ethics approval and consent to participate

All experiments involving animals were carried out in accordance with regulations (No. 5 proclamation of the Standing Committee of Hubei People's Congress) approved by the Standing Committee of the Hubei People's Congress in P. R. China. All animal sample collection procedures were approved by the Ethics Committee of Huazhong Agricultural University. All experimental procedures involving animals have awarded with a written consent from all participants and Jingpin farm of Huazhong Agricultural University.

Consent for publication

Not applicable.

Availability of data and materials

The datasets supporting the conclusions of this article are deposited in the NCBI SRA repository (https://www.ncbi.nlm.nih.gov/sra/), the accession number is PRJNA530644.

Competing interests

We declared this manuscript have no competing interests.

Funding

This work was supported by grants from the National Basic Research Program of China (2014CB138504) and China Agriculture Research System (CARS-35). The funding bodies did not participate in the design of the study, sample collection, analysis, or in the writing of the manuscript.

Author contributions

RWH designed the experimental study, carried out RT-qPCR, performed the bioinformatics analyses and edited manuscript. WSL contributed to collect sample and assist experiment. YYW involved in experimental design. WCL and YX involved in bioinformatics analyses. SYX contributed to collect sample, TTK involved in writing and editing. MGL provided a critical revision and approval of the article. All the authors read and approved the final manuscript.

Acknowledgements

We are very grateful to Mr. Jiang zongyong research group for providing Porcine trophectoderm cells (PTr2).

References

1. Ross JW, Ashworth MD, Stein DR, Couture OP, Tuggle CK, Geisert RD. Identification of differential gene expression during porcine conceptus rapid trophoblastic elongation and attachment to uterine luminal epithelium. Physiol Genomics. 2009;36:140–8.
2. Geisert RD, Schmitt R a. M. Early embryonic survival in the pig: Can it be improved? J Anim Sci. 2002;80 E-suppl_1:E54–65.
3. Bazer FW, Spencer TE, Johnson GA, Burghardt RC. Uterine receptivity to implantation of blastocysts in mammals. Front Biosci (Schol Ed). 2011;3:745–67.
4. Kyriazakis I, Whittemore CT. Whittemore's Science and Practice of Pig Production.
5. Keys JL, King GJ. Microscopic examination of porcine conceptus-maternal interface between days 10 and 19 of pregnancy. Am J Anat. 1990;188:221–38.
6. Ren Q, Guan S, Fu J, Wang A. Expression of tissue inhibitor of metalloproteinases-3 messenger RNA and protein in porcine endometrium during implantation. Molecular Biology Reports. 2011;38:3829–37.
7. Viganò P, Mangioni S, Pompei F, Chiodo I. Maternal-conceptus cross talk--a review. Placenta. 2003;24 Suppl B:S56-61.
8. Kurian NK, Modi D. Extracellular vesicle mediated embryo-endometrial cross talk during implantation and in pregnancy. J Assist Reprod Genet. 2019;36:189–98.
9. Bidarimath M, Khalaj K, Kridli RT, Kan FWK, Koti M, Tayade C. Extracellular vesicle mediated intercellular communication at the porcine maternal-fetal interface: A new paradigm for conceptus-endometrial cross-talk. Sci Rep. 2017;7:40476.
10. Nawaz M, Camussi G, Valadi H, Nazarenko I, Ekström K, Wang X, et al. The emerging role of extracellular vesicles as biomarkers for urogenital cancers. Nat Rev Urol. 2014;11:688–701.
11. Nguyen HPT, Simpson RJ, Salamonsen LA, Greening DW. Extracellular Vesicles in the Intrauterine Environment: Challenges and Potential Functions. Biol Reprod. 2016;95:109.
12. Nguyen HPT, Simpson RJ, Salamonsen LA, Greening DW. Extracellular Vesicles in the Intrauterine Environment: Challenges and Potential Functions. Biol Reprod. 2016;95:109.
13. Chen T, Xi Q-Y, Ye R-S, Cheng X, Qi Q-E, Wang S-B, et al. Exploration of microRNAs in porcine milk exosomes. BMC Genomics. 2014;15:100.
14. Zhao K, Liang G, Sun X, Guan LL. Comparative miRNAome analysis revealed different miRNA expression profiles in bovine sera and exosomes. BMC Genomics. 2016;17:630.
15. Huang X, Yuan T, Tschannen M, Sun Z, Jacob H, Du M, et al. Characterization of human plasma-derived exosomal RNAs by deep sequencing. BMC Genomics. 2013;14:319.
16. Vilella F, Moreno-Moya JM, Balaguer N, Grasso A, Herrero M, Martínez S, et al. Hsa-miR-30d, secreted by the human endometrium, is taken up by the pre-implantation embryo and might modify its transcriptome. Development. 2015;142:3210–21.
17. Lv C, Yu WX, Wang Y, Yi DJ, Zeng MH, Xiao HM. MiR-21 in extracellular vesicles contributes to the growth of fertilized eggs and embryo development in mice. Biosci Rep. 2018;38.

doi:10.1042/BSR20180036.

18. Kusama K, Nakamura K, Bai R, Nagaoka K, Sakurai T, Imakawa K. Intrauterine exosomes are required for bovine conceptus implantation. Biochem Biophys Res Commun. 2018;495:1370–5.
19. Qiao F, Ge H, Ma X, Zhang Y, Zuo Z, Wang M, et al. Bovine uterus-derived exosomes improve developmental competence of somatic cell nuclear transfer embryos. Theriogenology. 2018;114:199–205.
20. Burns G, Brooks K, Wildung M, Navakanitworakul R, Christenson LK, Spencer TE. Extracellular vesicles in luminal fluid of the ovine uterus. PLoS ONE. 2014;9:e90913.
21. Krawczynski K, Najmula J, Bauersachs S, Kaczmarek MM. MicroRNAome of porcine conceptuses and trophoblasts: expression profile of micrornas and their potential to regulate genes crucial for establishment of pregnancy. Biol Reprod. 2015;92:21.
22. Nie Z, Zhou F, Li D, Lv Z, Chen J, Liu Y, et al. RIP-seq of BmAgo2-associated small RNAs reveal various types of small non-coding RNAs in the silkworm, Bombyx mori. BMC Genomics. 2013;14:661.
23. Zhang B, Pan X, Cobb GP, Anderson TA. microRNAs as oncogenes and tumor suppressors. Dev Biol. 2007;302:1–12.
24. Rottiers V, Näär AM. MicroRNAs in metabolism and metabolic disorders. Nat Rev Mol Cell Biol. 2012;13:239–50.
25. Sarkar A, Volff J-N, Vaury C. piRNAs and their diverse roles: a transposable element-driven tactic for gene regulation? FASEB J. 2017;31:436–46.
26. Xia H, Mao Q, Paulson HL, Davidson BL. siRNA-mediated gene silencing *in vitro* and *in vivo*. Nature Biotechnology. 2002;20:1006–10.
27. Hu S-J, Ren G, Liu J-L, Zhao Z-A, Yu Y-S, Su R-W, et al. MicroRNA expression and regulation in mouse uterus during embryo implantation. J Biol Chem. 2008;283:23473–84.
28. Vilella F, Moreno-Moya JM, Balaguer N, Grasso A, Herrero M, Martínez S, et al. Hsa-miR-30d, secreted by the human endometrium, is taken up by the pre-implantation embryo and might modify its transcriptome. Development. 2015;142:3210–21.
29. Zhang L, Liu X, Liu J, Ma X, Zhou Z, Song Y, et al. miR-26a promoted endometrial epithelium cells (EECs) proliferation and induced stromal cells (ESCs) apoptosis via the PTEN-PI3K/AKT pathway in dairy goats. J Cell Physiol. 2018;233:4688–706.
30. Cheong AWY, Pang RTK, Liu W-M, Kottawatta KSA, Lee K-F, Yeung WSB. MicroRNA Let-7a and dicer are important in the activation and implantation of delayed implanting mouse embryos. Hum Reprod. 2014;29:750–62.
31. Bick JT, Flöter VL, Robinson MD, Bauersachs S, Ulbrich SE. Small RNA-seq analysis of single porcine blastocysts revealed that maternal estradiol-17beta exposure does not affect miRNA isoform (isomiR) expression. BMC Genomics. 2018;19:590.

32. Krawczynski K, Bauersachs S, Reliszko ZP, Graf A, Kaczmarek MM. Expression of microRNAs and isomiRs in the porcine endometrium: implications for gene regulation at the maternal-conceptus interface. BMC Genomics. 2015;16:906.
33. Flöter VL, Lorenz A-K, Kirchner B, Pfaffl MW, Bauersachs S, Ulbrich SE. Impact of preimplantational oral low-dose estradiol-17β exposure on the endometrium: The role of miRNA. Mol Reprod Dev. 2018;85:417–26.
34. Théry C, Witwer KW, Aikawa E, Alcaraz MJ, Anderson JD, Andriantsitohaina R, et al. Minimal information for studies of extracellular vesicles 2018 (MISEV2018): a position statement of the International Society for Extracellular Vesicles and update of the MISEV2014 guidelines. J Extracell Vesicles. 2018;7:1535750.
35. Hong L, Liu R, Qiao X, Wang X, Wang S, Li J, et al. Differential microRNA Expression in Porcine Endometrium Involved in Remodeling and Angiogenesis That Contributes to Embryonic Implantation. Front Genet. 2019;10:661.
36. Li W, Xi Y, Xue S, Wang Y, Wu L, Liu H, et al. Sequence analysis of microRNAs during pre-implantation between Meishan and Yorkshire pigs. Gene. 2018;646:20–7.
37. Galio L, Droineau S, Yeboah P, Boudiaf H, Bouet S, Truchet S, et al. MicroRNA in the ovine mammary gland during early pregnancy: spatial and temporal expression of miR-21, miR-205, and miR-200. Physiol Genomics. 2013;45:151–61.
38. Schanzenbach CI, Kirchner B, Ulbrich SE, Pfaffl MW. Can milk cell or skim milk miRNAs be used as biomarkers for early pregnancy detection in cattle? PLoS One. 2017;12. doi:10.1371/journal.pone.0172220.
39. Lv C, Yu WX, Wang Y, Yi DJ, Zeng MH, Xiao HM. MiR-21 in extracellular vesicles contributes to the growth of fertilized eggs and embryo development in mice. Biosci Rep. 2018;38. doi:10.1042/BSR20180036.
40. Li Z, Gou J, Jia J, Zhao X. MicroRNA-429 functions as a regulator of epithelial-mesenchymal transition by targeting Pcdh8 during murine embryo implantation. Hum Reprod. 2015;30:507–18.
41. Latifi Z, Fattahi A, Ranjbaran A, Nejabati HR, Imakawa K. Potential roles of metalloproteinases of endometrium-derived exosomes in embryo-maternal crosstalk during implantation. J Cell Physiol. 2018;233:4530–45.
42. Wang H, Matsumoto H, Guo Y, Paria BC, Roberts RL, Dey SK. Differential G protein-coupled cannabinoid receptor signaling by anandamide directs blastocyst activation for implantation. Proc Natl Acad Sci U S A. 2003;100:14914–9.
43. Mamo S, Mehta JP, McGettigan P, Lonergan P. 76 deciphering g-protein coupled receptor network during bovine conceptus development and maternal recognition of pregnancy. Reprod Fertil Dev. 2011;24:150–150.
44. Li Z, Jia J, Gou J, Zhao X, Yi T. MicroRNA-451 plays a role in murine embryo implantation through targeting Ankrd46, as implicated by a microarray-based analysis. Fertil Steril. 2015;103:834-834.e4.

45. Li X, Zhang W, Fu J, Xu Y, Gu R, Qu R, et al. MicroRNA-451 is downregulated in the follicular fluid of women with endometriosis and influences mouse and human embryonic potential. Reproductive Biology and Endocrinology. 2019;17:96.
46. Krawczynski K, Najmula J, Bauersachs S, Kaczmarek MM. MicroRNAome of Porcine Conceptuses and Trophoblasts: Expression Profile of microRNAs and Their Potential to Regulate Genes Crucial for Establishment of Pregnancy. Biol Reprod. 2015;92. doi:10.1095/biolreprod.114.123588.
47. Li R, Qiao J, Wang L, Li L, Zhen X, Liu P, et al. MicroRNA array and microarray evaluation of endometrial receptivity in patients with high serum progesterone levels on the day of hCG administration. Reprod Biol Endocrinol. 2011;9:29.
48. Gregory PA, Bert AG, Paterson EL, Barry SC, Tsykin A, Farshid G, et al. The miR-200 family and miR-205 regulate epithelial to mesenchymal transition by targeting ZEB1 and SIP1. Nat Cell Biol. 2008;10:593–601.
49. Zhao G, Yang C, Yang J, Liu P, Jiang K, Shaukat A, et al. Placental exosome-mediated Bta-miR-499-Lin28B/let-7 axis regulates inflammatory bias during early pregnancy. Cell Death & Disease. 2018;9:704.
50. Wang T, Wang G, Hao D, Liu X, Wang D, Ning N, et al. Aberrant regulation of the LIN28A/LIN28B and let-7 loop in human malignant tumors and its effects on the hallmarks of cancer. Molecular Cancer. 2015;14:125.
51. Su L, Liu R, Cheng W, Zhu M, Li X, Zhao S, et al. Expression patterns of microRNAs in porcine endometrium and their potential roles in embryo implantation and placentation. PLoS ONE. 2014;9:e87867.
52. Bazer FW, Thatcher WW. Theory of maternal recognition of pregnancy in swine based on estrogen controlled endocrine versus exocrine secretion of prostaglandin F2alpha by the uterine endometrium. Prostaglandins. 1977;14:397–400.
53. Piper MJ, Keynes RJ, Cook GM. Axon Guidance. In: eLS. American Cancer Society; 2012. doi:10.1002/9780470015902.a0000799.pub3.
54. Kawamura K, Kawamura N, Kumagai J, Fukuda J, Tanaka T. Tumor Necrosis Factor Regulation of Apoptosis in Mouse Preimplantation Embryos and Its Antagonism by Transforming Growth Factor Alpha/Phosphatidylionsitol 3-Kinase Signaling System. Biol Reprod. 2007;76:611–8.
55. Shi C, Han HJ, Fan LJ, Guan J, Zheng XB, Chen X, et al. Diverse endometrial mRNA signatures during the window of implantation in patients with repeated implantation failure. Hum Fertil (Camb). 2018;21:183–94.
56. Rosario FJ, Powell TL, Jansson T. Activation of placental insulin and mTOR signaling in a mouse model of maternal obesity associated with fetal overgrowth. Am J Physiol Regul Integr Comp Physiol. 2016;310:R87-93.
57. Li Z-H, Xiong Q-Y, Xu L, Duan P, Yang QO, Zhou P, et al. miR-29a regulated ER-positive breast cancer cell growth and invasion and is involved in the insulin signaling pathway. Oncotarget. 2017;8:32566–75.

58. Kim J-H, Kim K-A, Shin Y-J, Kim H, Majid A, Bae O-N. Methylglyoxal induced advanced glycation end products (AGE)/receptor for AGE (RAGE)-mediated angiogenic impairment in bone marrow-derived endothelial progenitor cells. J Toxicol Environ Health Part A. 2018;81:266–77.
59. Timofeeva AV, Chagovets VV, Drapkina YS, Makarova NP, Kalinina EA, Sukhikh GT. Cell-Free, Embryo-Specific sncRNA as a Molecular Biological Bridge between Patient Fertility and IVF Efficiency. Int J Mol Sci. 2019;20.
60. Wang Y, Hua R, Xue S, Li W, Wu L, Kang T, et al. mRNA/lncRNA expression patterns and the function of fibrinogen-like protein 2 in Meishan pig endometrium during the preimplantation phases. Molecular Reproduction and Development. 2019;:1–16.
61. Gao X, Ran N, Dong X, Zuo B, Yang R, Zhou Q, et al. Anchor peptide captures, targets, and loads exosomes of diverse origins for diagnostics and therapy. Sci Transl Med. 2018;10.
62. Deachapunya C, O'Grady SM. Regulation of chloride secretion across porcine endometrial epithelial cells by prostaglandin E2. J Physiol (Lond). 1998;508 (Pt 1):31–47.
63. Jaeger LA, Spiegel AK, Ing NH, Johnson GA, Bazer FW, Burghardt RC. Functional Effects of Transforming Growth Factor β on Adhesive Properties of Porcine Trophectoderm. Endocrinology. 2005;146:3933–42.
64. Zhang Q-L, Zhu Q-H, Zhang F, Xu B, Wang X-Q, Chen J-Y. Transcriptome-wide analysis of immune-responsive microRNAs against poly (I:C) challenge in Branchiostoma belcheri by deep sequencing and bioinformatics. Oncotarget. 2017;8:73590–602.
65. Langmead B, Trapnell C, Pop M, Salzberg SL. Ultrafast and memory-efficient alignment of short DNA sequences to the human genome. Genome Biol. 2009;10:R25.
66. Wang K, Liang C, Liu J, Xiao H, Huang S, Xu J, et al. Prediction of piRNAs using transposon interaction and a support vector machine. BMC Bioinformatics. 2014;15:419.
67. Friedländer MR, Chen W, Adamidi C, Maaskola J, Einspanier R, Knespel S, et al. Discovering microRNAs from deep sequencing data using miRDeep. Nat Biotechnol. 2008;26:407–15.
68. Xi Y, Liu H, Zhao Y, Li J, Li W, Liu G, et al. Comparative analyses of longissimus muscle miRNAomes reveal microRNAs associated with differential regulation of muscle fiber development between Tongcheng and Yorkshire pigs. PLoS ONE. 2018;13:e0200445.
69. 't Hoen PAC, Ariyurek Y, Thygesen HH, Vreugdenhil E, Vossen RHAM, de Menezes RX, et al. Deep sequencing-based expression analysis shows major advances in robustness, resolution and inter-lab portability over five microarray platforms. Nucleic Acids Res. 2008;36:e141.
70. Benjamini Y, Hochberg Y. Controlling the False Discovery Rate: A Practical and Powerful Approach to Multiple Testing. Journal of the Royal Statistical Society Series B (Methodological). 1995;57:289–300.

Tables

Due to technical limitations, tables are only available as a download in the supplemental files section.

Additional Files

Additional file 1: Table S1. Summary of sequencing data for each sample.

Additional file 2: Figure S1: Number distribution of total small RNAs. Pie chart demonstrates the mean distribution of different RNA species detected by small RNA-seq in all sequenced samples.

Additional file 3: Table S2. Summary of small RNAs (TPM >28 in at least one library).

Additional file 4: Table S3. Target genes of miRNAs.

Additional file 5: Figure S2. Principal component analysis of small RNAs. D10: day 10 of pregnancy; D13: day 13 of pregnancy; D18: day 18 of pregnancy.

Additional file 6: Table S4. Top 20 highly expressed known miRNAs.

Additional file 7: Table S5. KEGG analysis of target genes of top 20 highly expressed known miRNAs.

Additional file 8: Table S6. Differentially expressed miRNAs in comparisons of different stages.

Additional file 9: Table S7. Expression levels of DE miRNAs in three stages.

Additional file 10: Table S8. MiRNAs in Profile 6 of STEM.

Additional file 11: Table S9. MiRNAs in Profile 5 of STEM.

Additional file 12: Table S10. Primes of RT-qPCR.

Figures

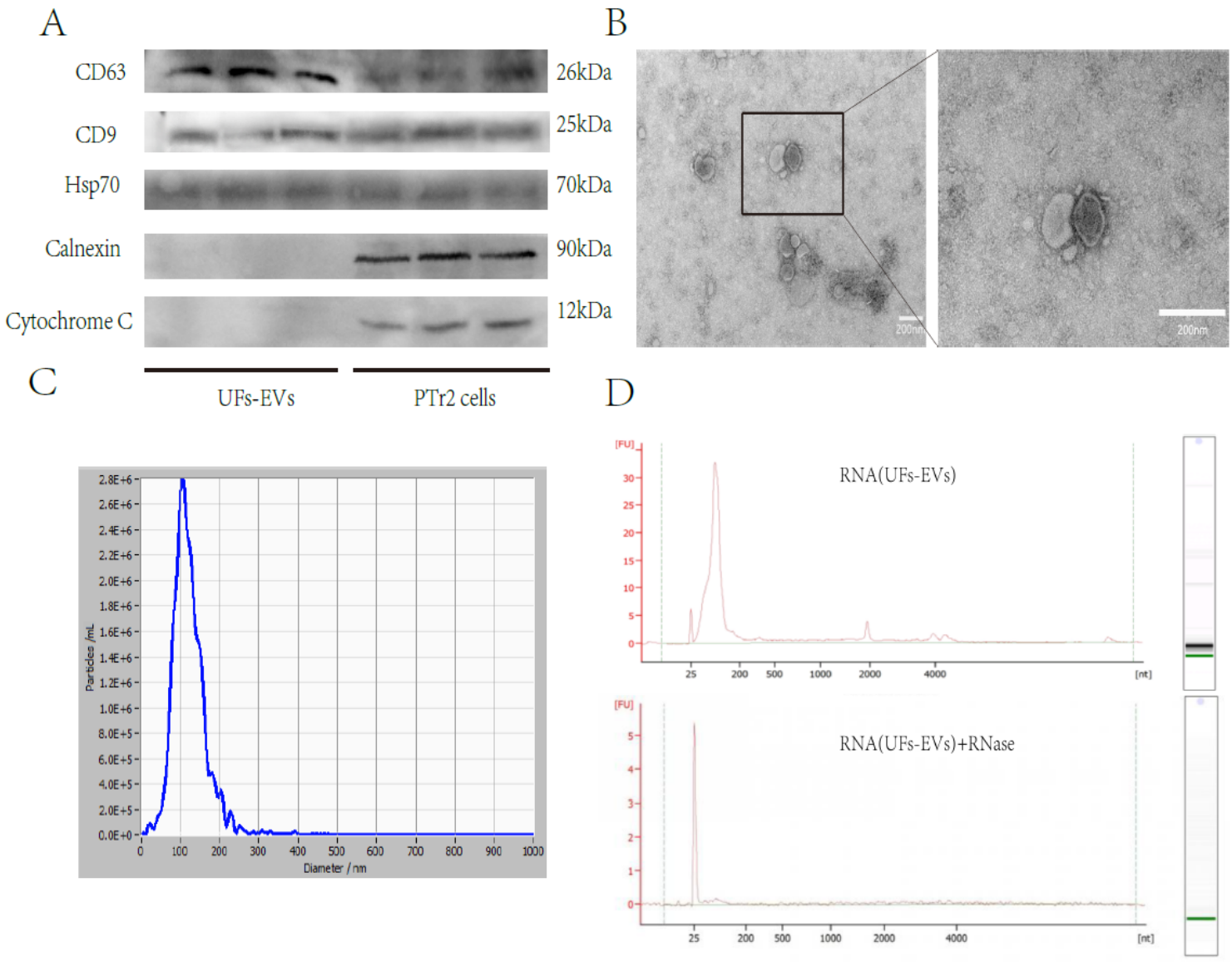

Figure 1

Characterization of EVs from porcine UFs. (A) Western Blotting detected exosomal markers CD63, CD9 and HSP70 in the UFs-EVs (EVs derived from porcine UFs) fraction as well as cellular fraction derived from PTr2 cells. Calnexin and Cytochrome C (negative control) were only detected in cell lysates of PTr2 cells. (B) Transmission electron microscopy (TEM) analysis of extracellular vesicles from porcine UFs, Scale bar = 200 nm. (C) Particle size of the extracellular vesicles from porcine UFs was measured by Nanoparticle tracking analysis (NTA). (D) Result from Agilent 2100 Bioanalyzer showing the RNA content of UFs-EVs with or without treatment with RNase A.

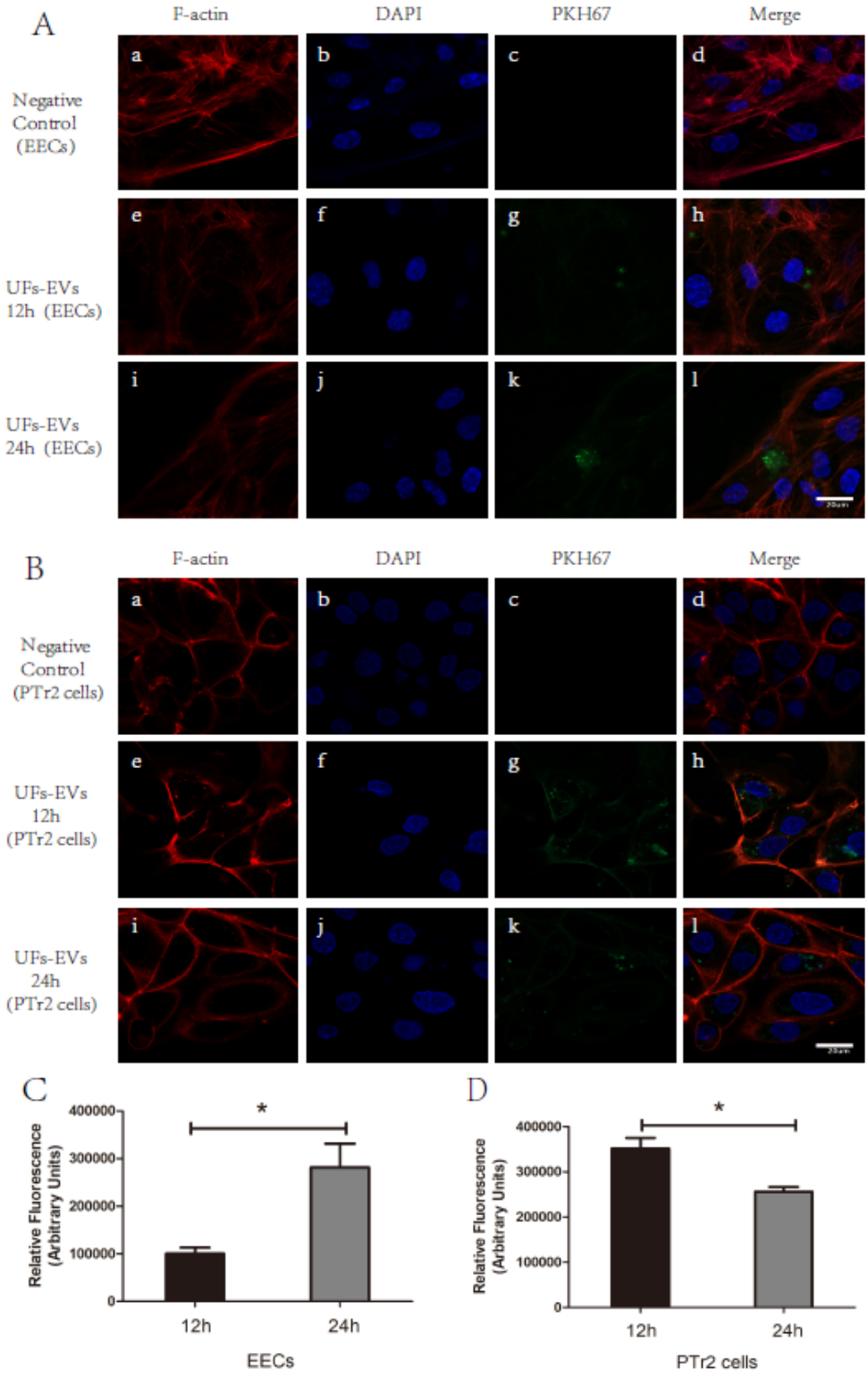

Figure 2

In vitro UFs-EVs uptake into EECs and PTr2 cells. (A, B) In vitro exosome uptake system using both EECs and PTr2 cells as recipients. Extracellular vesicles were isolated from porcine UFs, PKH67 labelled EVs (20 μg/mL) were added to EECs (A) or PTr2 cells (B) grown in cell culture plate and incubated for 12h (hours, e-h) and 24h (i-l) in a two set of experiments. EVs were successfully internalized by EECs and PTr2 cells in a time-dependent manner. Nuclei were stained with DAPI (blue: b, f, j); EVs were labelled with

PKH67 (green: g, k); Cellular F-actin were stained with TRITC Phalloidin (red: a, e, i). Control wells received the same preparation (PBS+PKH67) except for EVs(a-d), scale bar = 20 μm. Concentration of EVs uptake was measured by calculating the relative green fluorescence emitted by UFs-EVs in EECs (C) and PTr2 cells (D). Data are presented as mean ± SEM derived from three independent experiments.

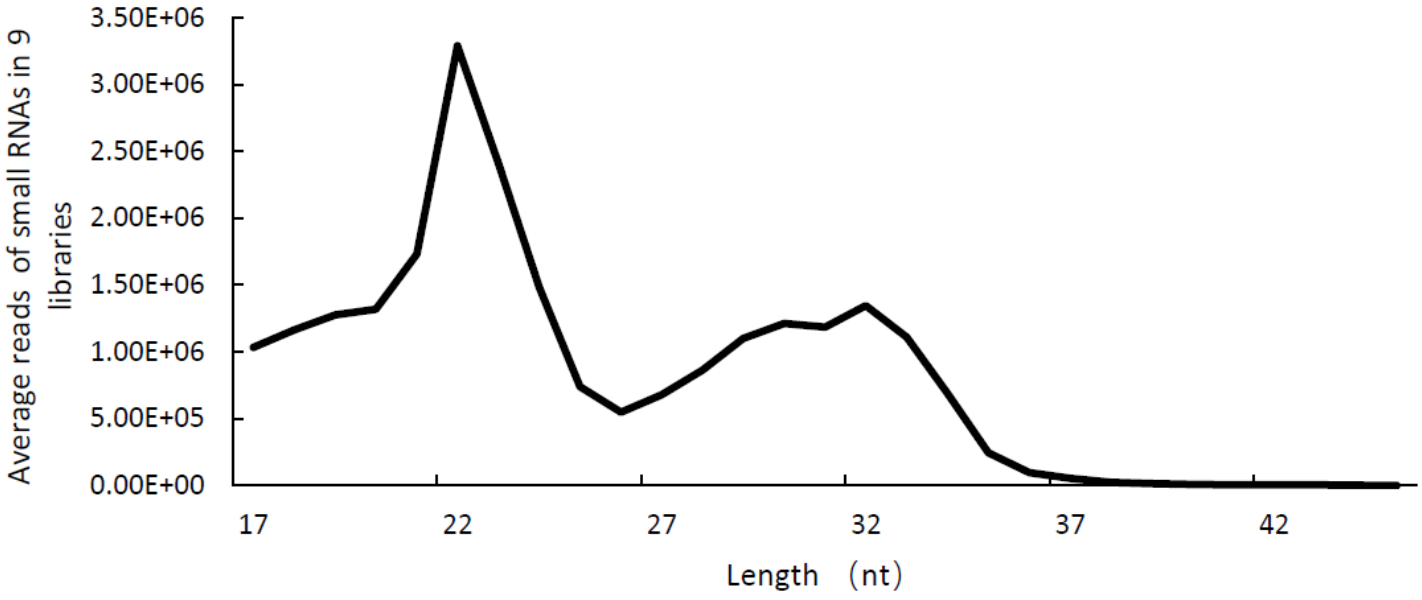

Figure 3

Sequence length distribution of small RNAs. nt: nucleotides.

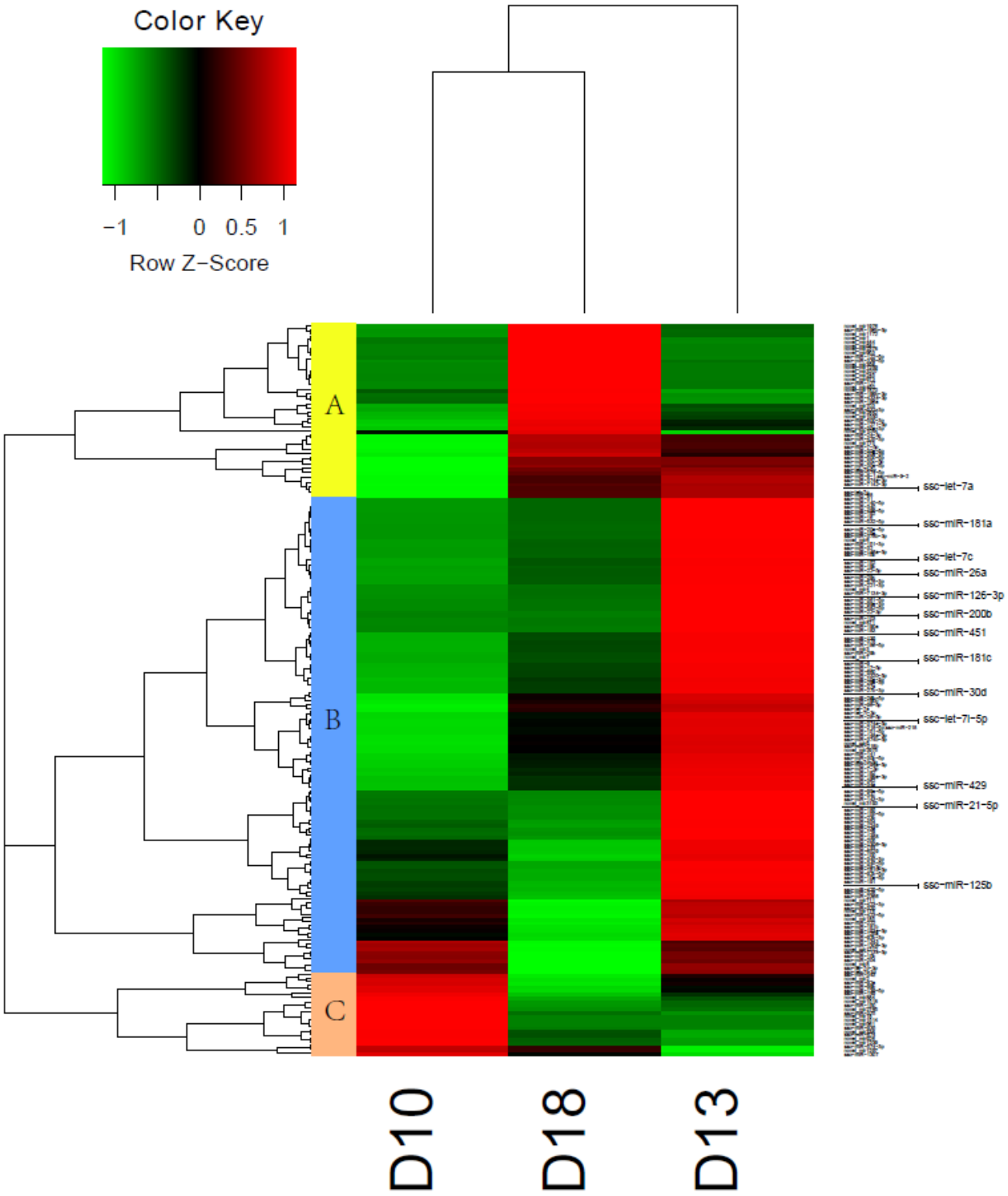

Figure 4

Hierarchical cluster analysis of miRNA expression. Emphasized miRNAs are indicated by arrows. D10: day 10 of pregnancy; D13: day 13 of pregnancy; D18: day 18 of pregnancy.

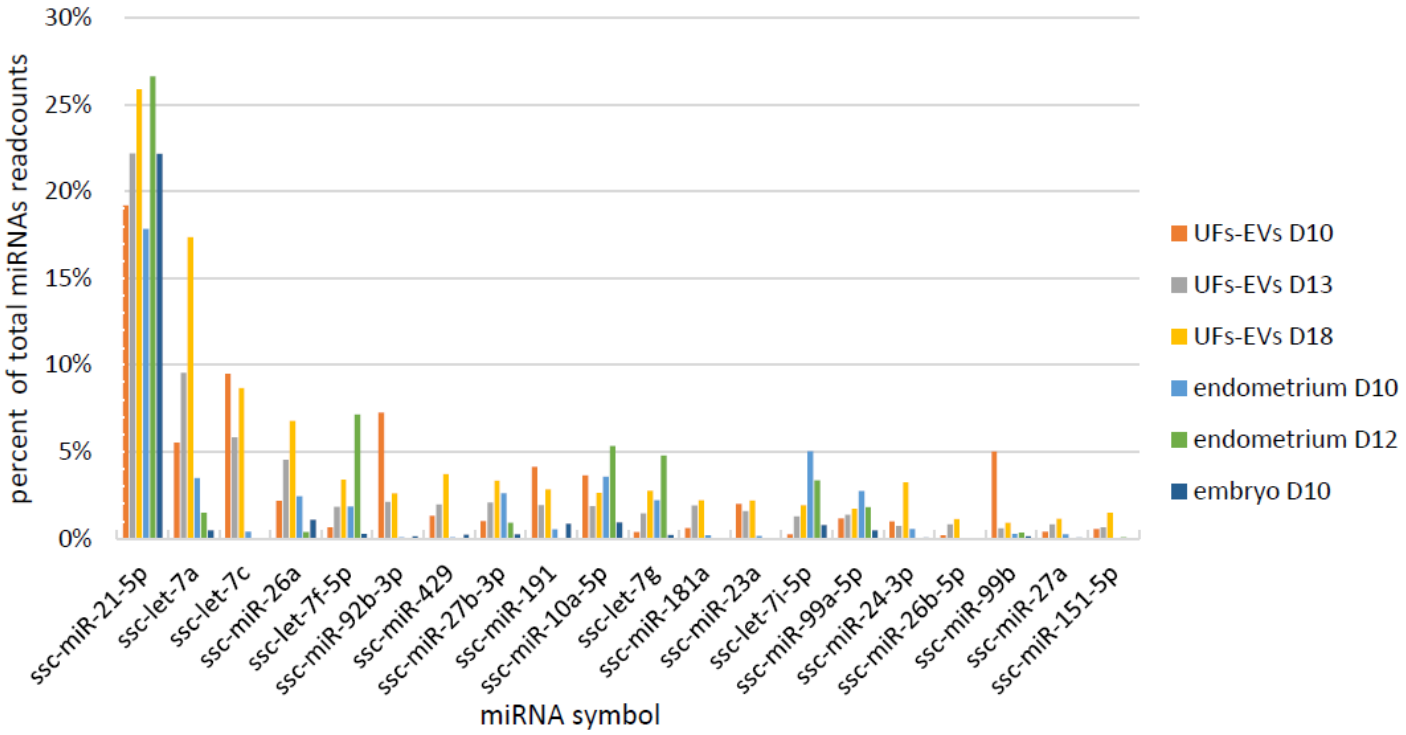

Figure 5

Top 20 most highly expressed miRNAs. D10: day 10 of pregnancy; D13: day 13 of pregnancy; D18: day 18 of pregnancy.

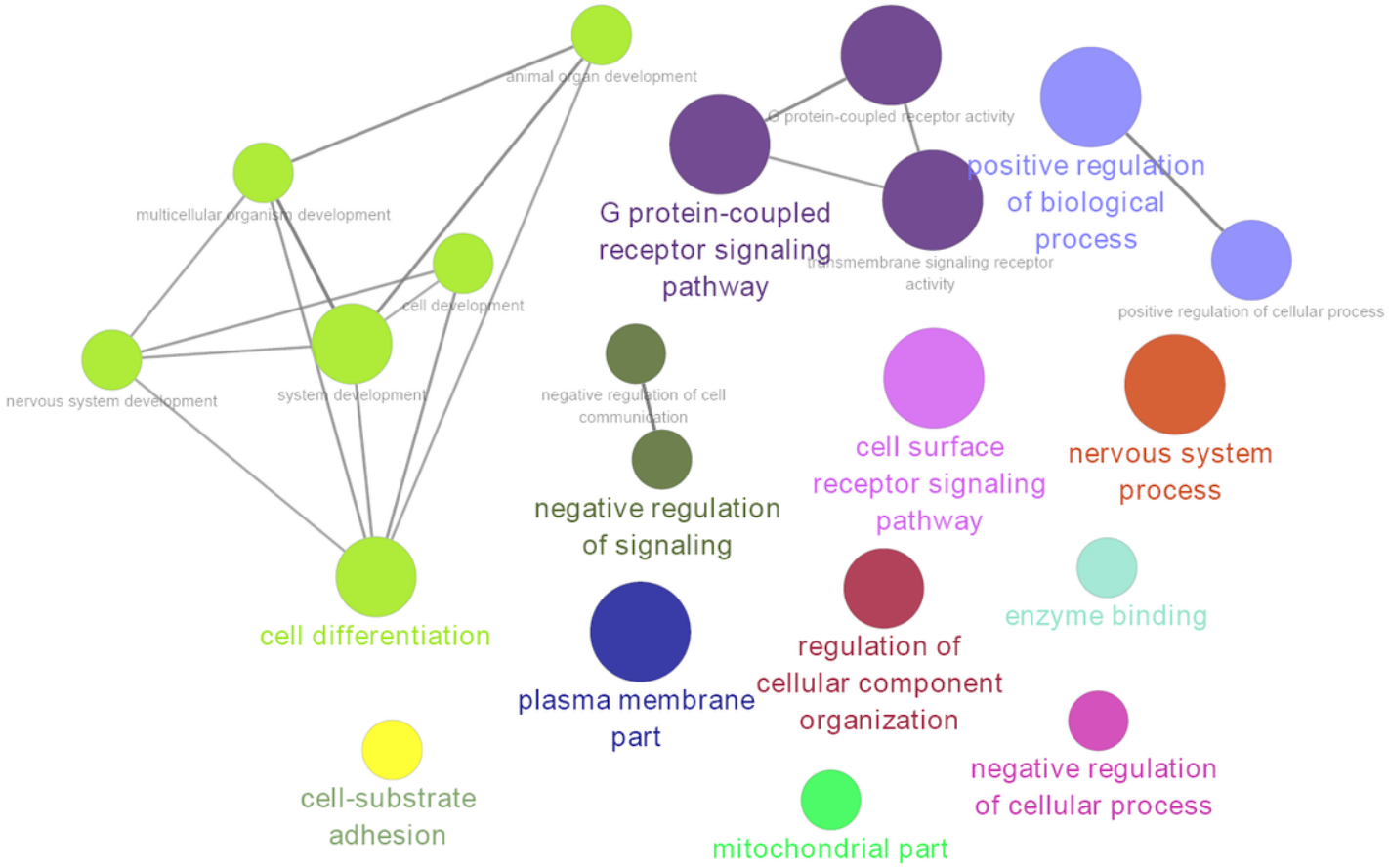

Figure 6

ClueGO network of GO terms. Each node represents a GO term. The class of GO term is reflected by the color of the nodes. Node size represents the enrichment significance of GO term.

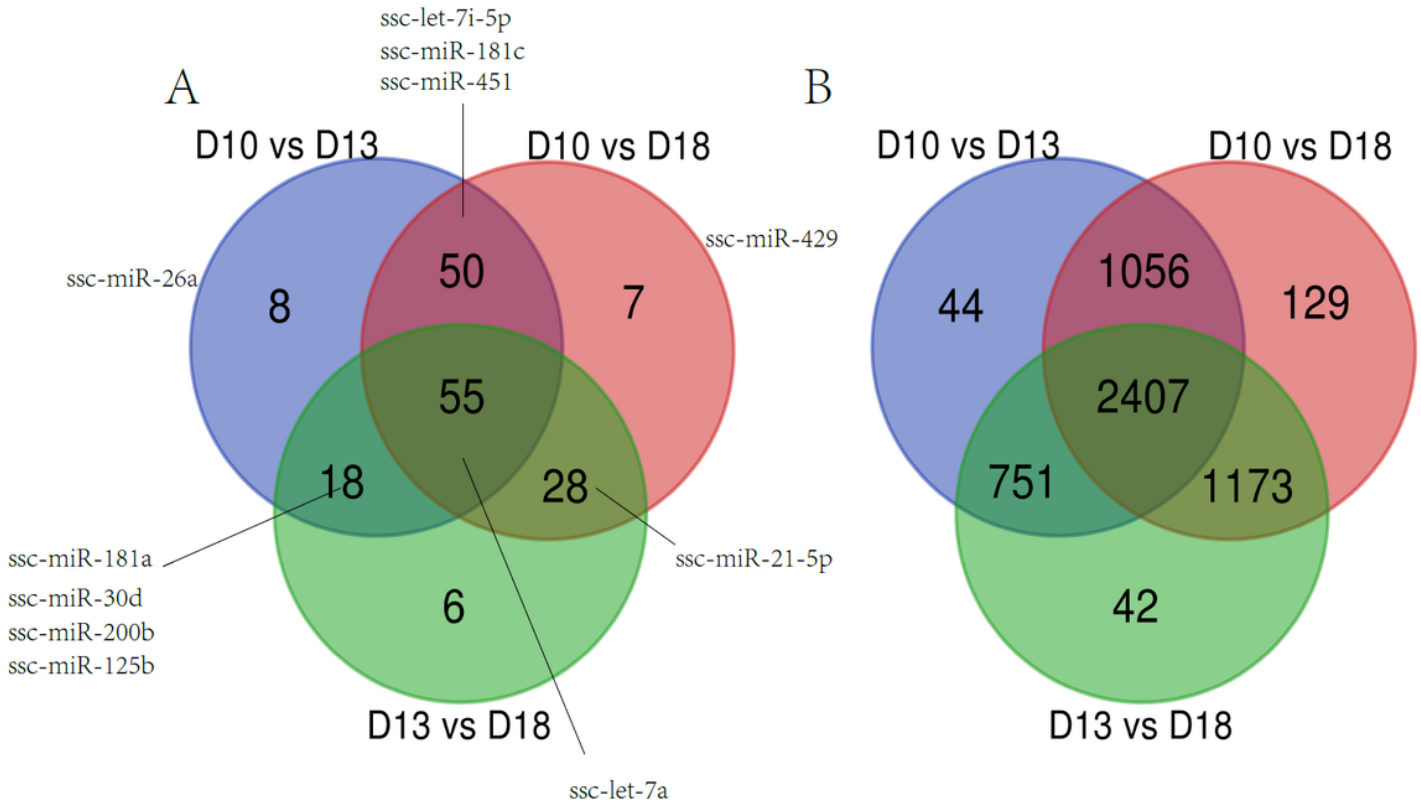

Figure 7

. (A) Differentially expression miRNAs. (B) Differentially expression piRNAs. The number marked in the overlapping colored areas indicates the common differentially expressed miRNAs between several groups. D10: day 10 of pregnancy; D13: day 13 of pregnancy; D18: day 18 of pregnancy.

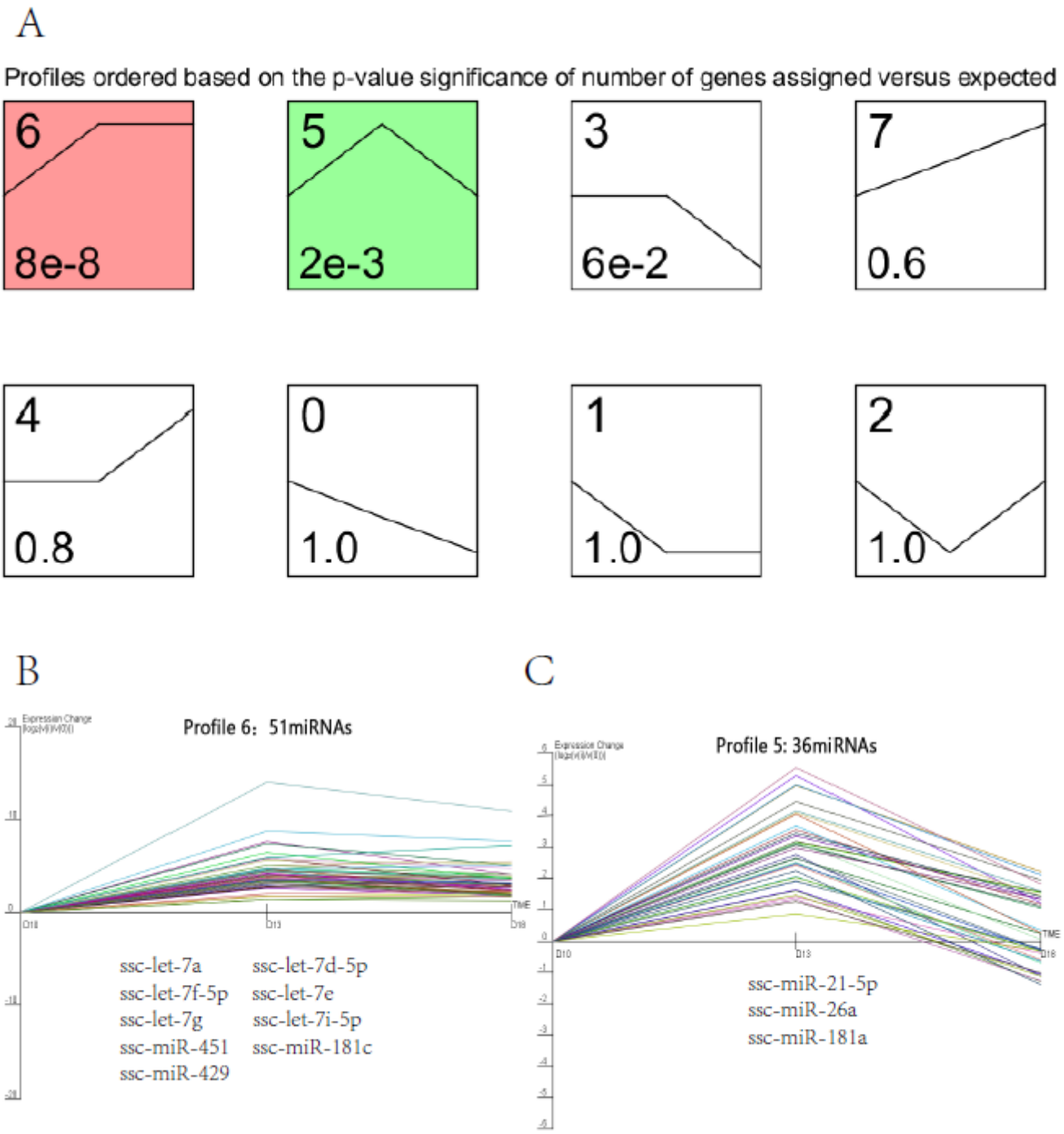

Figure 8

STEM clustering based on DE miRNAs. (A) Each square represents a kind of expression profile and colored squares mean statistical significance. The upper-left number in the box indicates the order of profile. The bottom-left number indicates the P-value. Polyline in the box presents the change pattern of miRNA expression levels. (B) (C) Detailed descriptions of miRNA expression patterns for “profile 6” and “profile 5”, respectively. D10: day 10 of pregnancy; D13: day 13 of pregnancy; D18: day 18 of pregnancy.

Figure 9

GO analysis of predicted target genes of DE miRNAs. D10: day 10 of pregnancy; D13: day 13 of pregnancy; D18: day 18 of pregnancy. “count”: the number of DE miRNAs.

Figure 10

KEGG analysis of predicted target genes of DE miRNAs. D10: day 10 of pregnancy; D13: day 13 of pregnancy; D18: day 18 of pregnancy. “count”: the number of DE miRNAs.

Supplementary Files

This is a list of supplementary files associated with this preprint. Click to download.

- Additionalfile8.xlsx
- Additionalfile2.pdf
- Additionalfile9.txt
- Additionalfile1.xlsx
- Additionalfile10.txt
- Additionalfile11.txt
- Table1.xlsx
- Additionalfile5.tif
- Additionalfile12.xlsx

- Additionalfile4.xlsx
- Additionalfile3.xlsx
- Additionalfile7.xlsx
- Checklist.docx
- Additionalfile6.xlsx